Geophys. J. R. astr. Soc. (1980) 62, 675–689

Anomalous geomagnetic variations and the concentration of telluric currents in south-west Queensland, Australia

D. V. Woods* and F. E. M. Lilley *Research School of Earth Sciences, Australian National University, Canberra, ACT 2600, Australia*

Received 1980 January 3; in original form 1979 September 21

Summary. A pattern of geomagnetic fluctuations in central Australia shown by a magnetometer array with instruments spaced at distances of order 100 km has been investigated in detail by a follow-up study in south-west Queensland with array instruments at distances of order 20 km apart. On a regional scale the pattern is simple and two-dimensional, and is evidently correlated with the spatial distribution of highly conducting sediments in the Great Artesian Basin of eastern Australia. Numerical studies of induction in two-dimensional models of the basin structure adequately account for the magnitude and scale of the observed regional pattern of anomalous fluctuation fields.

The smaller scale array disclosed details in the regional pattern for which interpretation proceeds in terms of current concentration in an equivalent current sheet. This sheet represents the integrated current flow in the upper 5 km of the crust, the maximum permissible depth of such a sheet current. The interpreted current distribution can be only partly explained by the known structure of the basin. Additional conductive structures must be present either within the basin or immediately below the basin in the basement rocks.

Taking into account knowledge of a conductivity anomaly in southern Australia, it is hypothesized that a current channel may exist from north to south across the Australian continent, joining the Gulf of Carpentaria to the Southern Ocean.

1 Introduction

The interpretation of geomagnetic fluctuation observations traditionally divides into two classes: those based on a one-dimensional earth (either radially symmetric or flat and horizontally layered), and those which indicate that local geology departs from one-dimensionality, and so is two- or three-dimensional.

*Present address: Department of Geological Sciences, Queen's University, Kingston, Ontario, Canada K7L 3N6.

The electromagnetic response of a one-dimensional earth is well known but the responses of general two-dimensional and three-dimensional earths are not calculable analytically unless simplifications are made; indeed the more complicated two-dimensional and especially three-dimensional cases are only tractable using numerical computer analysis. Nevertheless two- and three-dimensional induction situations can be recognized when they occur by certain parameters derived from the fluctuation data (e.g. Lilley 1974), and data from a magnetometer array will usually indicate whether induction has been observed over a structure of one, or more, dimensions, simply by the pattern of any anomaly observed.

Over the last 10 yr, particularly since the papers by Whitham & Andersen (1965), Dyck & Garland (1969) and Porath & Dziewonski (1971), increasing recognition has been given to the common occurrence of one particular aspect of three-dimensional induction, known variously as 'current channelling', 'current concentration' or 'current gathering'. This phenomenon is envisaged to occur when currents induced on a large, even global, scale flow locally in the region under observation essentially according to Ohm's law. Current channelling is perhaps one of the most simple results of three-dimensional induction, and also perhaps one of the most commonly observed. The flow of a uniform alternating current in a conductive channel according to Ohm's law requires that at least one transverse dimension of the conductor be less than its skin depth at the appropriate frequency. Under this condition the current flow is essentially 'quasi-direct'.

In this paper, current channelling is invoked to account for a distinctive geomagnetic fluctuation pattern found in south-west Queensland. Data from two magnetic variometer arrays are presented: a regional array in 1976 which discovered an anomaly particularly apparent in the vertical component of the fluctuation field, and a local array in 1977 which examined this anomaly in detail.

2 The observing sites

Fig. 1 shows the observing sites referred to in this paper, which are also listed with their geographic coordinates and geomagnetic declinations in Table 1. The 1976 array was initially sited to investigate the possibility of a northward extension to a conductivity anomaly found in southern Australia by the 1970 array (Gough, McElhinny & Lilley 1974). As shown in Fig. 1(b), the 1976 array straddles the western margin of the Great Artesian Basin of eastern Australia: to the south-east the array is over Mesozoic sedimentary platform cover and to the north-west it is over much older Proterozoic cratonic blocks and early Palaeozoic intracratonic basins.

The 1977 array was sited to examine in more detail an anomaly disclosed in the south-east corner of the 1976 array. The 1977 stations were taken as far east as site D1 in Fig. 1(c), in the hope of there recording a regional field remote from anomalous effects.

The instruments used in both array studies were the Gough–Reitzel variometers described by Lilley *et al.* (1975). A variety of data were secured with both operations, many events being recorded successfully in all components by all instruments. The events recorded varied from pulsations with periods of about 1 min, to polar magnetic substorms of approximately 1 hr duration, to quiet daily variations with periods of up to 1 day. An interpretation of some of the data from the western part of the 1976 array has been given by Woods & Lilley (1979), on the basis of one-dimensional geologic structure.

3 Vertical-field response arrows

Fig. 2 shows vertical-field response arrows, both in-phase and quadrature, for all stations occupied in central Australia. The arrows have been estimated using standard least-squares

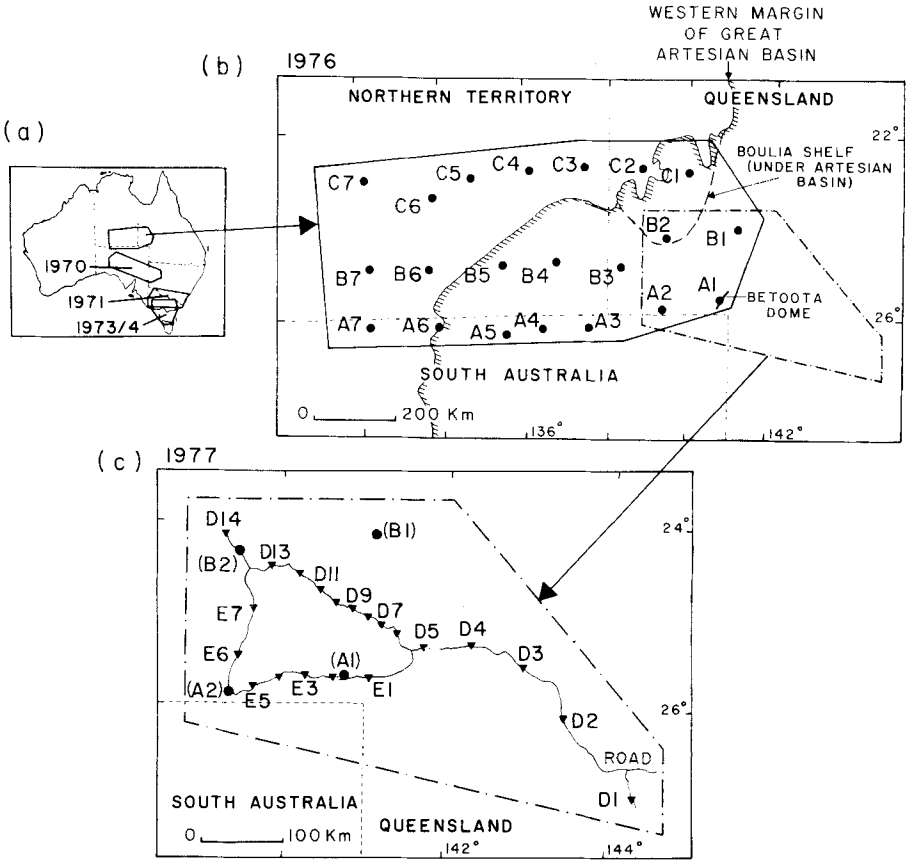

Figure 1. Observing sites of the 1976 and 1977 magnetometer arrays in central Australia and south-west Queensland. Included in (b) are three geological features, taken from Geological Society of Australia (1971) and Senior, Mond & Harrison (1978): (i) The approximate surface expression of the western margin of the Great Artesian Basin; the sediments of the basin shelve deeper towards the south-east from this boundary. (ii) The position of the buried 'Boulia Shelf', which is a major structure in the basement of the Artesian Basin. (iii) The 'Betoota Dome', one of a number of local structures known in the Artesian Basin.

procedures (Woods 1979) to obtain the best fit of a variety of recorded magnetic events to the relationship

$$Z = AX + BY$$

where all quantities are complex and may vary with frequency; X, Y and Z are Fourier transforms of the records of the horizontal north, east and vertically-down magnetic fluctuation components. The parameters A and B should be governed only by the electrical conductivity structure of the earth within the 'induction area' of the observations (Lilley & Bennett 1973). Arrows have been determined for a range of periods from 10 to 100 min; those for 50 min are shown in Fig. 2 as being representative of the range. At least four individual substorm events with widely differing horizontal source-field polarizations were used in the response arrow determinations.

Table 1.

Observing sites for the 1976 array in central Australia

Code	Station	Abbreviation	Latitude	Longitude	Declination
A1	Mt. Leonard	MLD	25°38'S	140°47'E	6°50'E
A2	Birdsville	BVL	25°55'	139°20'	6°26'
A3	Poolarranna	PLR	26°19'	137°33'	5°58'
A4	Mokari	MKR	26°19'	136°26'	5°37'
A5	Dalhousie Springs	DHS	26°26'	135°29'	5°19'
A6	Tieyon	TYN	26°13'	133°52'	4°50'
A7	Ernabella	ERN	26°15'	132°10'	4°20'
B1	Davenport Downs	DVP	24°09'	141°06'	6°44'
B2	Bedourie	BDR	24°21'	139°27'	6°18'
B3	Muncoonie	MNC	25°04'	138°20'	6°02'
B4	Geosurveys Hill	GSY	24°59'	136°48'	5°37'
B5	Riecks Dam	RKD	25°02'	135°27'	5°14'
B6	Idracowra	IDR	25°04'	133°43'	4°44'
B7	Angas Downs	ANG	25°02'	132°16'	4°19'
C1	Boulia	BOL	22°55'	139°53'	6°15'
C2	*Glenormiston*	GLN	22°53'	138°49'	5°57'
C3	Marqua	MQA	22°49'	137°21'	5°34'
C4	Jervois	JRV	22°54'	136°08'	5°16'
C5	Mt. Riddock	MRK	23°02'	134°41'	4°53'
C6	Bond Springs	BNS	23°31'	133°50'	4°40'
C7	Derwent	DRW	23°09'	132°10'	4°13'

Observing sites for the 1977 array in southwest Queensland

Code	Station	Abbreviation	Latitude	Longitude	Declination
D1	Bulloo	BUL	26°56'S	144°20'E	8°02'E
D2	Thylungra	THY	26°06'	143°26'	7°39'
D3	Moothandella	MTH	25°33'	142°56'	7°26'
D4	Whitula	WHT	25°20'	142°17'	7°13'
D5	Gidya	GDY	25°22'	141°43'	7°03'
D6	Carrick	CRK	25°14'	141°23'	6°56'
D7	Farrar	FRR	25°09'	141°13'	6°53'
D8	Round Mt.	RND	25°03'	141°01'	6°49'
D9	Carbine	CBN	24°59'	140°51'	6°46'
D10	Diamantina	DIA	24°54'	140°40'	6°42'
D11	Gibber Plain	GIB	24°46'	140°28'	6°38'
D12	Germachie	GER	24°35'	140°11'	6°31'
D13	Sand Ridge	SND	24°27'	139°49'	6°25'
D14	Pipeline	PIP	24°09'	139°16'	6°14'
E1	Tarcarara	TAR	25°43'	141°02'	6°55'
E2	Pierikoola	PKL	25°42'	140°34'	6°47'
E3	Durrie	DUR	25°40'	140°15'	6°41'
E4	Clay Pan	CLY	25°43'	139°56'	6°35'
E5	Roseberth	ROS	25°49'	139°37'	6°31'
E6	Moonies Grave	MON	25°31'	139°26'	6°25'
E7	Koolivoo	KOO	24°59'	139°38'	6°25'

3.1 THE 1976 ARROWS

The 1976 in-phase arrows point to the south-east in a uniform pattern over a remarkably wide area, indicating that the strongest vertical-field fluctuations occur when the horizontal-field fluctuations are polarized north-west to south-east. This result indicates the presence of a good electrical conductor in the ground in the vicinity of the south-east part of the array, with its longitudinal dimension approximately at right angles to the direction of the arrows.

One station (A1) in the extreme south-east of the 1976 array shows a reversal from the common in-phase arrow direction. Such a reversal implies that telluric current is concentrated between station A1 and the other 1976 stations, rather like a line current with a reversal in the vertical component of its magnetic field from one side of the line to the other.

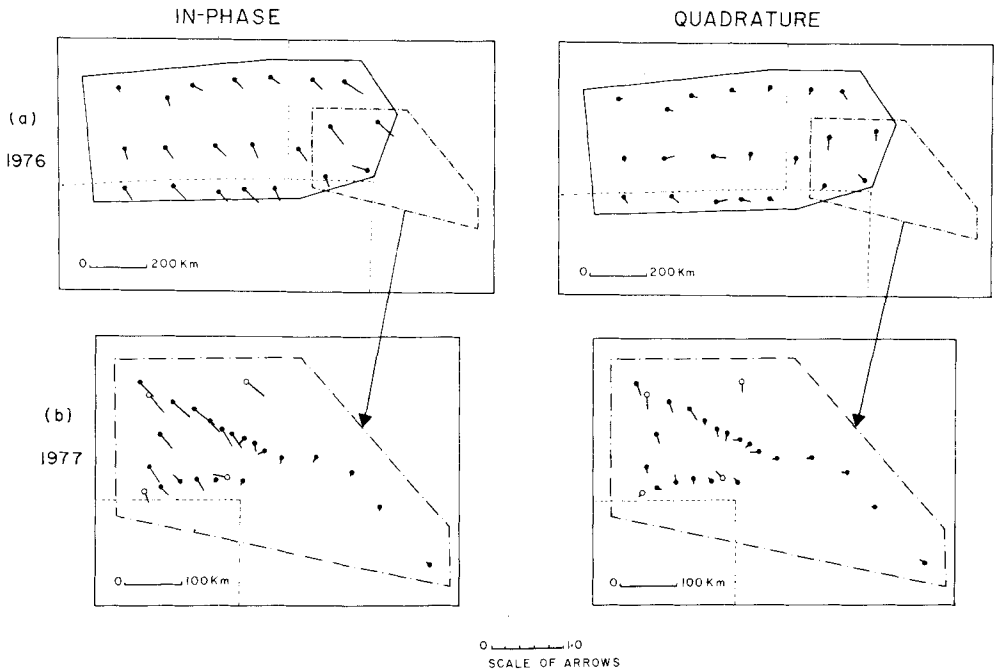

Figure 2. Vertical-field response arrows (also known as Parkinson vectors and induction arrows) for the 1976 and 1977 arrays in central Australia. The arrows are for disturbances of period 50 min, and have a typical error circle of diameter 0.1 arrow units.

3.2 THE 1977 ARROWS

Fig. 2(b) shows arrows obtained in a detailed study of the reversal of Fig. 2(a). These arrows do not confirm the simple reversal pattern of a line current but are more complicated. Isolated reversals are present, but the overall pattern is one of decreased arrow-length east of station D9, with some additional local variability of length and direction. This general pattern is more typical of the response over the edge of a conductive sheet (analogous perhaps with the pattern which would be observed by a common coast-effect traverse if it were continued out to sea) and does not fit a simple line current model.

In some cases the reversals and other sharp changes in arrow length or direction occur over distances of order 20 km. This length-scale indicates that the conductive structures causing these anomalous effects must be at depths of order 20 km or less. Furthermore, the zones of anomalous conductivity must be confined to lateral dimensions of the same scale or less, in order to account for the isolated nature of some of the anomalous arrows (*cf.* stations A1 and E4).

3.3 INTERPRETATION

The geographic pattern of vertical-field response arrows presented in Fig. 2 suggests electromagnetic induction in the sedimentary rocks of the Great Artesian Basin as their cause. Not only does the Artesian Basin have the basic geometry of a sheet, but the porous sedimentary rocks which form it have very low resistivities averaging from 1 to 20 ohm m. The Artesian Basin is known to shelve from its north-west margin deeper to the south-east, which may explain the wide areal extent of the pattern of 1976 arrows pointing south-east. Two-dimensional induction in a basin model is presented in Section 4.

The second-order anomalies found by the 1977 array may be related to structures in the basement of the Artesian Basin. Indeed such features are known to be present from seismic and other geophysical exploration and to a first approximation appear to correlate with the anomalous vertical-field response arrows. For example the reversed arrow at station A1 is coincident with a well-documented basement structure referred to as the 'Betoota Dome' and marked on Fig. 1(b) (the correlation is discussed further in Section 6).

4 Inductive response of a two-dimensional basin model

To test the hypothesis that electromagnetic induction in the conductive sediments of the Great Artesian Basin can account for the general pattern of the response arrows in Fig. 2, two-dimensional modelling of the electromagnetic response of basin-shaped conductivity structures was carried out using computational procedures adapted from Jones & Pascoe (1971) and Pascoe & Jones (1972). Fig. 3 shows two simple basin sections: the first with an abrupt edge, and the second with a shelving edge to approximate the western margin of the Great Artesian Basin, (an actual cross-section of the Great Artesian Basin is shown in Fig. 7 below). Electrical conductivities of the sedimentary and underlying basement rocks were obtained from surface resistivity, borehole resistivity, and magnetotelluric surveys reported by Whiteley & Pollard (1971) and Moore *et al.* (1977) (see also Middleton 1979).

The results of such model computations (especially for the shelving model) are in agreement with the general pattern of the observed response from the 1976 array, giving comparable vertical-field amplitudes, in terms of a unit horizontal-field, as the vertical-field response arrows shown in Fig. 2(a) for both in-phase and quadrature cases. Thus two-dimensional induction in the basin is adequate to account for the regional pattern of the

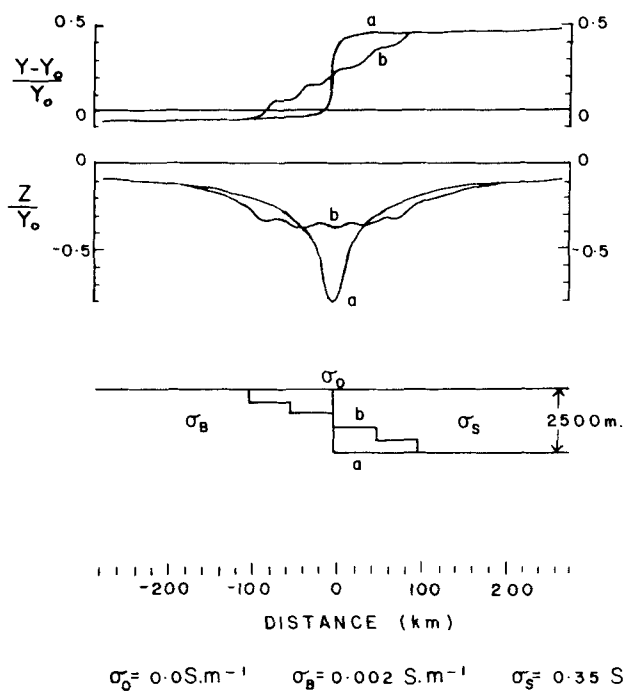

Figure 3. Two-dimensional models of the edge of a sedimentary basin and their computed in-phase anomalous magnetic fields at a period of 48 min.

observed fluctuation fields. However, two-dimensional induction in the basin does not account for the small-scale features shown by the 1977 arrows. Additional conductive structures must be present in the vicinity of these features, either within the basin sediments or within the basement rocks immediately below the basin.

Rather than modelling more complex two-dimensional structures to find a fit to the anomalous fields, interpretation now proceeds by determining a pattern of quasi-direct currents which will give the observed magnetic fields (a recent discussion of this approach is given by Banks 1979). This procedure is adopted particularly as the 1977 data themselves exhibit some of the diagnostic features of current-channelling, as will now be demonstrated.

5 Detailed analysis of the 1977 array data

5.1 STACKED PROFILES

An example of the data recorded by the 1977 array is given in Fig. 4(a), which shows the basic records of a substorm event reduced and resolved to geographic coordinates. The differing characteristics of the Z-traces such as the small response at stations D1 to D8, E1 and E2, and the reversal at station E4 can be seen to correspond with the arrow pattern of Fig. 2(b).

5.2 DIFFERENCE PROFILES

Fig. 4(b) shows the results of subtracting, from the records of Fig. 4(a), the appropriate component as recorded at station D1. Station D1 is chosen as the best available estimate of the regional variation field as it is the most easterly station and so is most remote from the anomaly. The differences of Fig. 4(b) thus obtained are similar to the differences of Babour *et al.* (1976) and Babour & Mosnier (1977), though the resolution of the instruments used here is less, and the distance over which the subtracted profile is taken as representing the regional field is greater.

The differences in Fig. 4(b) have varying amplitudes but essentially similar morphology, indicating that as anomalous signals they occur in-phase (or antiphase) everywhere across the 1977 array. Only one example is presented here but similar results hold for other events. As pointed out by Babour *et al.* (1976), this natural separation of the anomalous fields into independent functions of space and time is a distinctive characteristic of channelled current.

5.3 HODOGRAPHS

The horizontal components of the event shown in Fig. 4 are displayed as hodographs (traces of the horizontal fluctuation vector in map form) in Fig. 5. Fig. 5(a) shows the full event plotted out, and Fig. 5(b) shows the differences of each station with station D1. The linear nature of the traces in Fig. 5(b) demonstrates the correlation between the horizontal components of the anomalous field. This correlation holds even though the X to Y amplitude ratio varies from station to station thereby changing the direction of the linear hodographs. The circular nature of the difference hodographs at the most northern stations may indicate the inadequacy of subtracting, as the regional field there, the field recorded at station D1.

The linear nature of the anomalous fields in Fig. 5(b) relative to the circular nature of the regional fields in Fig. 5(a), and the fact that the same linear hodographs are produced by the anomalous fields of other events with different regional fields, is a further demonstration of the current channelling nature of the anomalous fields. The direction of each of the linear

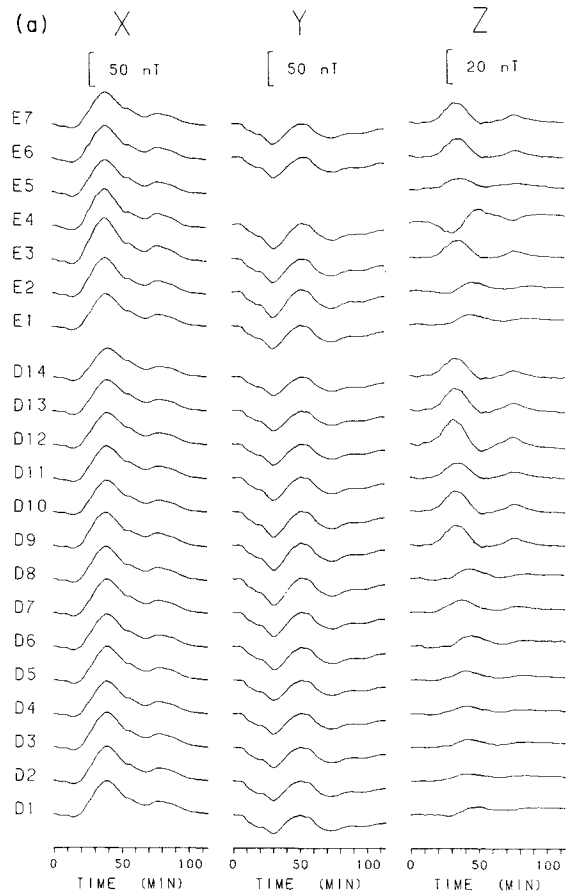

Figure 4. (a) Simultaneous recordings of a substorm event from the 1977 array. The records commence at 1105 UT, 1977 September 13. (b) The data of (a) when the records of station D1 are subtracted as being estimates of a regional field.

hodographs in Fig. 5(b) can be taken as the orientation of the anomalous horizontal fields at the station, and its perpendicular is then the direction of anomalous current flow in the ground near that station.

6 Current channelling analysis

6.1 ANOMALOUS-FIELD PROFILES ACROSS STRIKE

Peak amplitudes relative to some arbitrary zero (commonly taken as the level at the start of the event) have been scaled off the difference records, as exemplified in Fig. 4(b), for a number of events from the 1977 array. Such peak amplitudes are effectively simultaneous across the array, consistent with the anomalous fields being in-phase at all stations and in all components. Thus a measure of peak amplitudes gives a measure of the anomalous fields at some particular time.

The horizontal components of the anomalous fields have then been resolved to a set of axes parallel (and perpendicular) to the average direction of the linear, anomalous-field hodographs plotted for each event and exemplified in Fig. 5(b). This direction, 25° south of

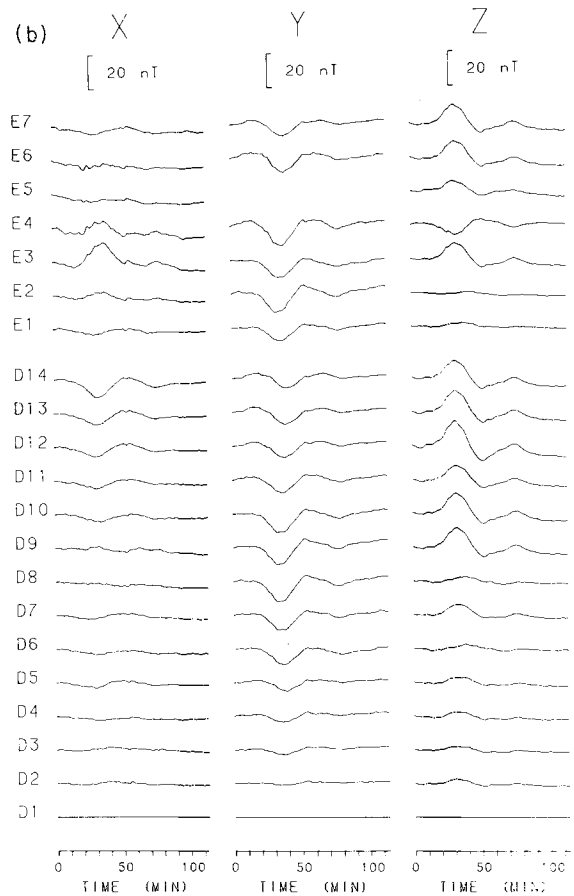

east, is approximately parallel to the D-line of stations. The component resolved parallel to this line will be denoted Y', reckoned positive to the south-east, and the orthogonal component, X', will be reckoned positive to the north-east.

Plotting these components, as well as the anomalous vertical fields, from stations D1 to D14 along the D-line produces profiles of the total horizontal (Y') and vertical (Z) fields as shown in Fig. 6(a). For a simple current flow in the X' direction, the X' magnetic field profile should be uniformly zero across the region; its increase in Fig. 6(a) from south-east to north-west may be due to an increase of the regional field from south to north, typical of substorms originating in the southern auroral zone. The irregularity of the X' profile at station D9 may indicate a localized change of direction of the ground currents near that station, as is evident from the anomalous-field hodographs in Fig. 5(b).

As with the hodographs, different events produce similar results. The shapes of anomalous-field, across-strike profiles for other events in a period range from 10 min to 2 hr are effectively the same as depicted in Fig. 6(a), with only the vertical scale changing. This observation indicates that to a first approximation the electric currents in the earth flow coherently through the 1977 array area, consistently in the same geographic positions and orientations, independent of source fields configuration and, to within the limits stated, independent of frequency.

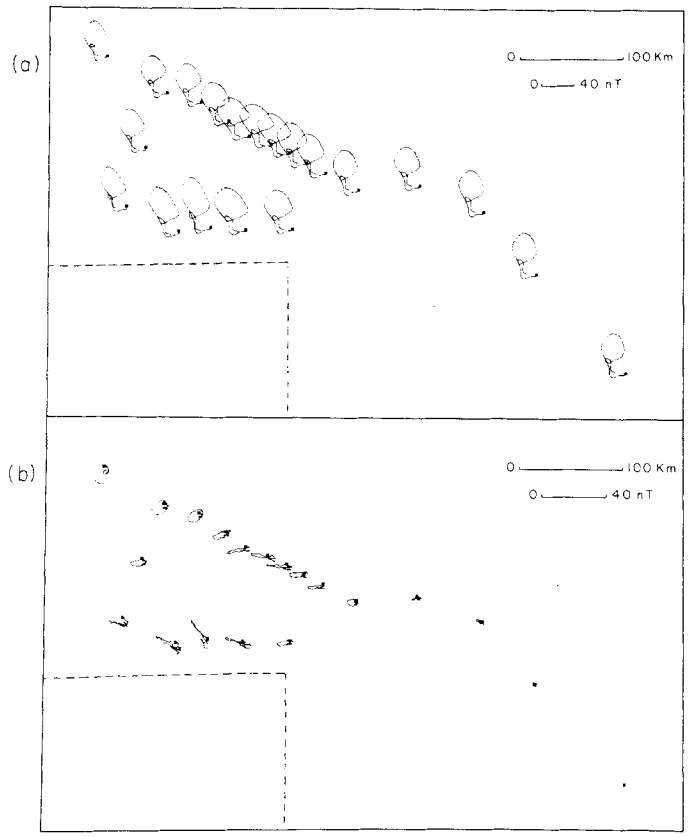

Figure 5. Hodographs for the horizontal field fluctuations shown in Fig. 4. (a) As recorded and shown in Fig. 4(a). (b) With the D1 records subtracted from each station as a regional field, as shown in Fig. 4(b).

6.2 CURRENT INVERSION

The observations of Fig. 6(a) are now interpreted in terms of a steady current sheet flowing at some depth below the surface. The current sheet is considered to be flowing in the $+X'$ direction (25° east of north) and to be comprised of a finite number of infinite-length current elements. The magnetic field above a single such current element can be calculated from the Biot–Savart law and the total horizontal or vertical field at any point on the surface can be expressed as a linear combination of all fields from all current elements. If the number of points, at which the total field is known, is greater than or equal to the number of current elements then a direct matrix inversion of the field will produce a distribution of current in the ground. (This procedure is discussed in more detail in Appendix A.)

The anomalous fields shown in Fig. 6(a) were thus interpreted, and the resultant current distributions and their magnetic fields are shown in Fig. 6(b–e). A number of different techniques were employed to produce smoothed or physically more significant solutions. Five of these techniques, which are described more fully in Woods (1979), are:

(i) increasing the number of points for inversion by smoothed interpolation and extrapolation of the basic data points;

(ii) adjusting the baseline of the Z data by 3.5 nT to equalize the positive and negative areas of the Z-profile;

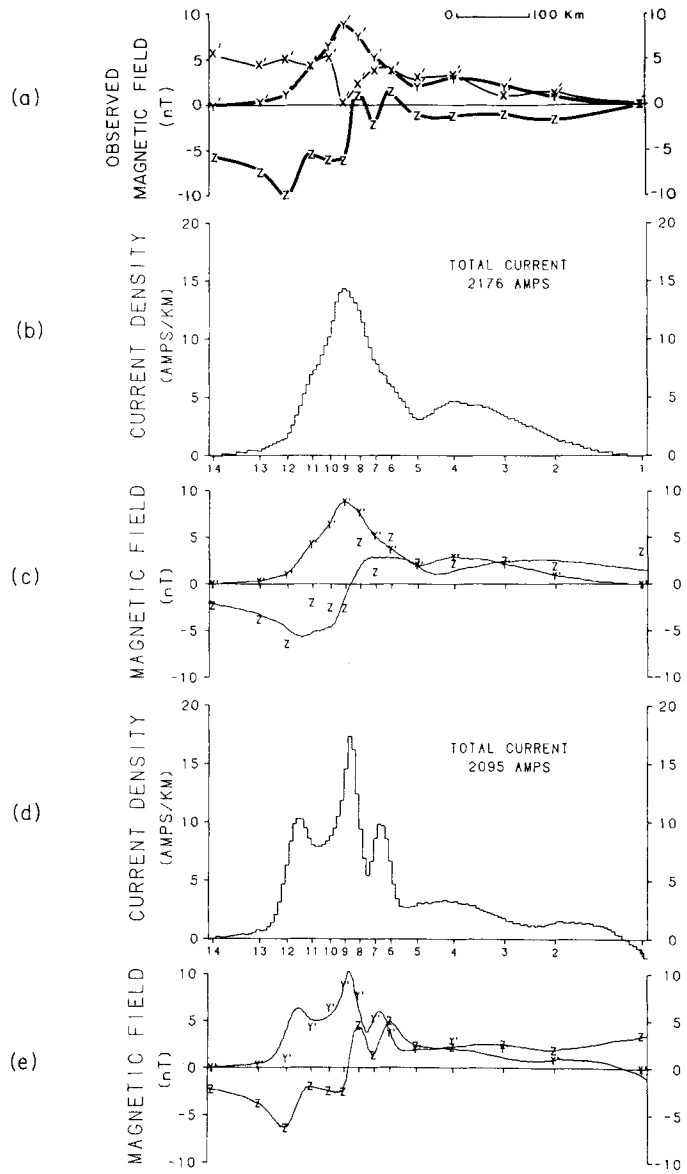

Figure 6. (a) Instantaneous amplitudes of the resolved horizontal (X' and Y') and vertical (Z) fluctuation fields as recorded at approximately 1550 UT 1977 September 23 along the line from stations D14 to D1. (b) Current sheet solution from inversion of Y' data. (c) Fit of Y' solution to Y' data and Z data. (d) Current sheet solution from inversion of Z data. (e) Fit of Z solution to Y' data and Z data. The numbers on the horizontal axes in (b) and (d) refer to stations on the D-line, and show the positions of these stations along the traverse.

(iii) considering current elements to be adjoining ribbons instead of separated lines, thus allowing smooth solutions to be found at shallow depths;

(iv) offsetting the current elements from the data points for a Z solution, as an element makes no contribution to the Z field directly above it; and

(v) smoothing each initial 'exact', but somewhat irregular, solution with a running mean.

6.3 RESULTS

Current distributions have thus been obtained for model conducting sheets at different depths below the D-line traverse. As is to be expected from potential field theory, solutions at greater depths show sharper variations of current with distance across the traverse. For sheets at depths greater than 10 km reversed current is required in places to produce a fit to the observed vertical-field data along the D-line. Zones of reversed current are physically implausible, and so a maximum depth of order 10 km for such a current sheet solution is obtained. Since the anomalous field has greater variability along the E-line, as can be seen in Fig. 4(b), the maximum depth of a reasonable (unidirectional) sheet current solution determined there is considerably less, of order 5 km.

The current distributions shown in Fig. 6(b and d) have the same general form, but the vertical-field solution (Fig. 6d) displays second-order features which are absent from the horizontal-field solution (Fig. 6b). However, the vertical-field solution produces a better fit to the observed horizontal field, than the horizontal-field solution to the observed vertical field. Since the vertical field above a shallow concentration of current has wider lateral extent than the horizontal field, and since the vertical component can be either positive or negative depending on the position of observation, whereas the horizontal component is always positive, there is a greater probability of observing shallow concentrations of current density with the vertical component. Hence, the vertical-field solution is interpreted to be a truer representation of the actual current pattern in the ground: the horizontal solution represents a smoothed average. Localized changes in the direction of the sheet current, as seen by the difference hodographs in Fig. 5(b), may have a minor effect on the current solutions but will not alter them substantially.

The general pattern of the current distributions shown in Fig. 6 may be reflecting the structure of the Great Artesian Basin as shown by the geological cross-section in Fig. 7, particularly south-east of station D6. However, the greater current density between stations D6 and D12, and the second-order features of the vertical-field solution, cannot be accounted for by the basin alone. Additional conductors within or beneath the basin are causing currents to be concentrated in this part of south-west Queensland.

Some of the second-order details of the vertical-field current solution are correlatable to known structures in the basement rocks. In particular the sharp low in current density between stations D7 and D8, seen in Fig. 6(d), lies along strike of the 'Betoota' basement dome at station A1, referred to in Section 3.3. The basement high does not completely pinch out the overlying current-carrying sediments but conductors at the flanks of the dome, due possibly to faulting, may gather current away from the top of the dome to beneath stations D6–D7 and D8–D9.

The peak in current density beneath stations D11–D12 is approximately coincident with a basement structure known as the 'Boulia Shelf', as inferred from aeromagnetic data. This structure is thought to represent the faulted contact between Palaeozoic rocks to the east

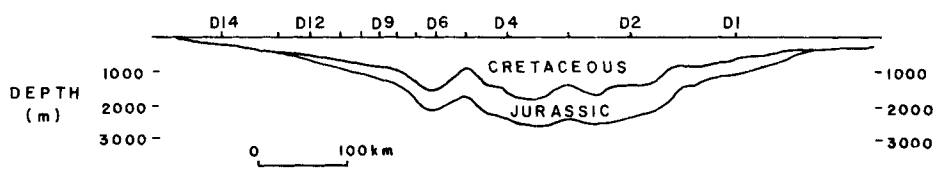

Figure 7. Geologic cross-section of the Great Artesian Basin along the D-line of stations shown in Fig. 1. (This part of the Artesian Basin is known as the Eromanga Basin, and its section as shown here is after Senior *et al.* 1978.)

and Precambrian rocks to the west and is marked to the north by faulting in the overlying sediments. Gravity data from this part of south-west Queensland also show a linear feature parallel with the Boulia Shelf though offset to the south-east. This feature appears coincident with the peak in current at stations D8–D9 and has been interpreted as representing another thrust-faulted contact between two different rock types (Rumph 1978).

7 Conclusion

The most straightforward interpretation of magnetometer fluctuation data recorded in south-west Queensland appears to be that magnetic activity induces a concentration of current to flow coherently through the Great Artesian Basin. Localized features of this current flow may reflect channelling of the induced currents into conductive structures in the basement rocks beneath the basin.

Two-dimensional induction models of the Artesian Basin account for the general pattern of the observed anomalous magnetic fluctuations. Simple models of current flow in a two-dimensional section of the basin sediments partly account for observed fields in south-west Queensland but do not explain the interpreted sharp concentrations of currents. Additional conductive structures in the basement rocks are required to explain these features.

The currents flowing across south-west Queensland may connect with the conductivity anomaly mapped by the 1970 array in southern Australia, and this conductor may in turn have an electrical link with the Southern Ocean (Garland 1975). If, to the north of the 1977 array area, the position of current concentration continues to follow the western edge of the Artesian Basin then it will meet the seas north of Australia in the Gulf of Carpentaria. A current path may thus be completed right across the Australian continent, linking the oceans to north and south.

Surface measurements of telluric currents or magnetometer measurements in boreholes might provide valuable supplementary information, to the extent of providing some estimate of the current actually flowing in the sediments during a magnetic fluctuation event.

Acknowledgments

This paper describes work carried out at the Australian National University during the tenure by one of us (DVW) of a research scholarship there. In the field operation of the two magnetometer arrays, essential help and much hospitality has been received from many people, to all of whom the authors express their thanks. We acknowledge particularly the contributions of Brian Smith and Jan Styles during the 1976 array operation, and those of Jim Leven, David Mainprice and Linda Woods during the 1977 array operation. Merren Sloane has assisted widely with instrument preparation, data reduction, and the drafting of diagrams. The projects have been encouraged and supported by A. L. Hales, M. W. McElhinny and A. E. Ringwood.

References

Babour, K. & Mosnier, J., 1977. Differential geomagnetic sounding, *Geophysics*, **42**, 66–76.

Babour, K., Mosnier, J., Daignieres, M., Vasseur, G., Le Mouel, J. L. & Rossignol, J. C., 1976. A geomagnetic variation anomaly in the Northern Pyrenees, *Geophys. J. R. astr. Soc.*, **45**, 583–600.

Banks, R. J., 1979. The use of equivalent current systems in the interpretation of geomagnetic deep sounding data, *Geophys. J. R. astr. Soc.*, **56**, 139–157.

Dyck, A. V. & Garland, G. D., 1969. A conductivity model for certain features of the Alert anomaly in geomagnetic variations, *Can. J. Earth Sci.*, **6**, 513–516.

Garland, G. D., 1975. Correlation between electrical conductivity and other geophysical parameters, *Phys. Earth planet. Interiors*, **10**, 220–230.

Geological Society of Australia, 1971. *Tectonic Map of Australia and New Guinea*, 1:5,000,000, Sydney.

Gough, D. I., McElhinny, M. W. & Lilley, F. E. M., 1974. A magnetometer array study in southern Australia, *Geophys. J. R. astr. Soc.*, **36**, 345–362.

Jones, F. W. & Pascoe, L. J., 1971. A general computer program to determine the perturbation of alternating electric currents in a two-dimensional model of a region of uniform conductivity with an embedded inhomogeneity, *Geophys. J. R. astr. Soc.*, **24**, 3–30.

Lilley, F. E. M., 1974. Analysis of the geomagnetic induction tensor, *Phys. Earth planet. Interiors*, **8**, 301–316.

Lilley, F. E. M. & Bennett, D. J., 1973. Linear relationships in geomagnetic variation studies, *Phys. Earth planet. Interiors*, **7**, 9–14.

Lilley, F. E. M., Burden, F. R., Boyd, G. W. & Sloane, M. N., 1975. Performance tests of a set of Gough–Reitzel magnetic variometers, *J. Geomagn. Geoelectr.*, **27**, 75–83.

Middleton, M. F., 1979. Correlation between well log and surface resistivity measurements – a case study in the Eromanga Basin, Queensland, *Bull. Aust. Soc. Explor. Geophys.*, **10**, 176–178.

Moore, R. F., Kerr, D. W., Vozoff, K. & Jupp, D. L. B., 1977. Southern Cooper Basin magneto-telluric survey, South Australia, 1974, *Bureau of Mineral Resources, Geology and Geophysics, Canberra, Australia, Record* 1977/41.

Pascoe, L. J. & Jones, F. W., 1972. Boundary conditions and calculation of surface values for the general two-dimensional electromagnetic induction problem, *Geophys. J. R. astr. Soc.*, **27**, 179–193.

Porath, H. & Dziewonski, A., 1971. Crustal resistivity anomalies from geomagnetic deep sounding studies, *Rev. Geophys. Space Phys.*, **9**, 891–915.

Rumph, B., 1978. Regional gravity and magnetic data of the Central Eromanga Basin area: implications on the crustal structure, regional geology and tectonic history, *MSc thesis*, University of Sydney, Sydney.

Senior, B. R., Mond, A. & Harrison, P. L., 1978. Geology of the Eromanga Basin, *Bureau of Mineral Resources, Geology and Geophysics, Canberra, Australia, Bullentin* 167.

Whiteley, R. J. & Pollard, P. C., 1971. A combined deep resistivity and magnetotelluric sounding in the Eromanga Basin, Queensland, *Search*, (ANZAAS), **2**, 103–105.

Whitham, K. & Andersen, F., 1965. Magneto-telluric experiments in northern Ellesmere Island, *Geophys. J. R. astr. Soc.*, **10**, 317–345.

Woods, D. V., 1979. Geomagnetic depth sounding studies in central Australia, *PhD thesis*, Australian National University, Canberra.

Woods, D. V. & Lilley, F. E. M., 1979. Geomagnetic induction in central Australia, *J. Geomagn. Geoelectr.*, **31**, 449–459.

Appendix A: direct matrix inversion of anomalous magnetic field profiles to obtain a sheet current distribution

The direct inversion of anomalous magnetic fields to give a current distribution in the ground will generally produce a non-unique solution, due to the basic properties of magnetic potential fields. However, it is possible to make certain assumptions about the anomalous telluric currents and thereby apply restrictions which force a unique solution. The assumptions made in Section 6.2 of the paper above to interpret the anomalous magnetic fields in south-west Queensland are that (1) the anomalous currents are flowing everywhere in phase and so are quasi-direct, (2) the currents are strictly two-dimensional, and (3) the currents are concentrated in a single plane at depth d below the surface. The relevance of the first two assumptions is demonstrated in the paper and the third assumption is made upon the basis of the known geometry of the sedimentary-basin conductivity-structure in south-west Queensland.

The assumed two-dimensional sheet current is considered to be composed of a number of current elements, all of infinite length. The magnetic field above a single such current

element can then be calculated by the Biot–Savart law

$$\mathbf{B} = \frac{\mu_0}{4\pi}\int \frac{I\,\mathbf{dl} \times \mathbf{r}}{r^2}$$

where $I\,\mathbf{dl}$ is a small element of current, $\mathbf{r}$ is the position vector of the element relative to the observation point and $\mathbf{B}$ is the magnetic induction field. For a line element the horizontal and vertical components of the magnetic field on the ground surface, above a line current of strength I buried at depth d, are:

$$B_y(y) = \frac{\mu_0 I}{2\pi}\,\frac{d}{y^2 + d^2}$$

$$B_z(y) = \frac{\mu_0 I}{2\pi}\,\frac{y}{y^2 + d^2}$$

where y is the horizontal offset of the point of observation from the line current, and μ_0 is the permeability of free space. Generalizing to an arbitrary origin of position, so that $y = y_0 - y_i$ where y_0 is the observation position and y_i is the line current position, and then normalizing by the depth so that $p = y_0/d$ and $q = y_i/d$ gives:

$$B_y(p) = \frac{\mu_0 I}{2\pi d}\,\frac{1}{1 + (p-q)^2}$$

$$B_z(p) = \frac{\mu_0 I}{2\pi d}\,\frac{(p-q)}{1 + (p-q)^2}$$

Magnetic fields add vectorially hence the total horizontal magnetic field at any point on the surface (say at position p_k as the kth point of n distinct observation points) can be expressed as a linear combination of all fields from all current elements, i.e.

$$B_y(p_k) = \frac{\mu_0}{2\pi d}\sum_{j=1}^{m}\frac{I_j}{1 + (p_k - q_j)^2}$$

where the horizontal field at point p_k is due to the summed effects of m different current elements at positions q_j, $(j = 1, 2, \ldots, m)$. A similar expression holds for the vertical field observed at p_k.

Given observations (or interpolations) of the actual horizontal field strengths B_y at different points p_k, the equation immediately above then represents a system of linear equations which can be written in matrix notation as

$$\mathbf{b}_k = \mathbf{A}_{jk} \cdot \mathbf{x}_j$$

where A_{jk} is an $m \times n$ coefficient matrix containing elements $1/[1 + (p_k - q_j)^2]$, b_k is a column matrix with (known) elements $B_y(p_k)2\pi d/\mu_0$, and x_j is the solution matrix containing the current elements I_j. If $m < n$ the solution can be computed using a standard least-squares matrix inversion algorithm. Thus current elements of strengths I_j are obtained which at depth d and horizontal positions q_j account for the observed horizontal magnetic field strengths $B_y(p_k)$ at surface positions p_k; and similarly for the interpretation of observed vertical magnetic field strengths.